chemistry

MDPI

Article

Structures of Three Alkaline-Earth Metal Germanides Refined from Single-Crystal X-ray Diffraction Data

Nian-Tzu Suen and Svilen Bobev *

Department of Chemistry and Biochemistry, University of Delaware, Newark, DE 19716, USA
* Correspondence: bobev@udel.edu

Abstract: The calcium- and strontium- alumo-germanides $Sr_xCa_{1-x}Al_2Ge_2$ ($x \approx 0.4$) and $SrAl_2Ge_2$ have been synthesized and structurally characterized. Additionally, a binary calcium germanide CaGe has also been identified as a byproduct. All three crystal structures have been established from single-crystal X-ray diffraction methods and refined with high accuracy and precision. The binary CaGe crystallizes with a CrB-type structure in the orthorhombic space group *Cmcm* (no. 63; $Z = 4$; Pearson symbol *oC*8), where the germanium atoms are interconnected into infinite zigzag chains, formally $[Ge]^{2-}$. The calcium atoms are arranged in monocapped trigonal prisms, centered by Ge atoms. $Sr_xCa_{1-x}Al_2Ge_2$ ($x \approx 0.4$) and $SrAl_2Ge_2$ have been confirmed to crystallize with a $CaAl_2Si_2$-type structure in the trigonal space group $P\bar{3}m1$ (no. 164; $Z = 1$; Pearson symbol *hP*5), where the germanium and aluminum atoms form puckered double-layers, formally $[Al_2Ge_2]^{2-}$. The calcium atoms are located between the layers and reside inside distorted octahedra of Ge atoms. All presented structures have a valence electron count satisfying the octet rules (e.g., $Ca^{2+}Ge^{2-}$ and $Ca^{2+}[Al_2Ge_2]^{2-}$) and can be regarded as Zintl phases.

Keywords: crystal structure; germanides; Zintl phases

Citation: Suen, N.-T.; Bobev, S. Structures of Three Alkaline-Earth Metal Germanides Refined from Single-Crystal X-ray Diffraction Data. *Chemistry* **2022**, *4*, 1429–1438. https://doi.org/10.3390/chemistry4040094

Received: 11 October 2022
Accepted: 29 October 2022
Published: 2 November 2022

1. Introduction

Prior work by our laboratory has covered the structural elucidation for a number of binary and ternary germanides [1–12]. We have identified numerous new compounds, proving the *M*–*X*–Ge systems (*M* = alkali, alkaline-earth or rare-earth metals, *X* = *p*-block element) to be a fertile ground for new materials discovery. Many new structures, all solved and refined from single-crystal X-ray diffraction data, have resulted from these studies and have brought new knowledge on this somewhat unusual chemistry, where the germanium atoms are in a mildly reduced state.

We have also studied the substitution patterns of metals with different valences, which has demonstrated the ability of some germanides to accommodate substitutions and wider valence electron count while maintaining their global structural integrity. Good examples of the latter approach, and its effects on the electronic structure, site preference, and magnetic properties, are the extended series $RE_{5-x}Ca_xGe_4$ (orthorhombic Gd_5Si_4-type structure) and $RE_{5-x}Ca_xGe_3$ (tetragonal Cr_5B_3-type structure or hexagonal Mn_5Si_3-type structure) [13–15]. In some of these cases, the structures have been found to exist in relatively large parts of the compositional space, suggesting that the chemical bonding could be continuously varied based on the number of available valence electrons. In other cases, curiously, the homogeneity range appears to be limited, and the formed structures only exist for a specific amount of available valence electrons. Relevant examples here are $REAl_{1-x}Ge_3$ (*RE* = Nd, Sm, Gd, Tb, Dy, Ho; $0.6 < x < 0.9$) [5]; $REAl_{1-x}Ge_2$ (*RE* = Gd–Tm, Lu, Y; $0.8 < x < 0.9$) [8]; $SrAl_{4-x}Ge_x$, $BaAl_{4-x}Ge_x$, and $EuAl_{4-x}Ge_x$ ($x \approx 0.3$–0.4) [4], among others. In further instances, it was found that the valence electron count is not sufficient to stabilize a given structure, such as $M_3In_2Ge_4$ and $M_5In_3Ge_6$ (*M* = Ca, Sr, Eu, and Yb) [9]; and $(Eu_{1-x}Ca_x)_4In_3Ge_4$ and $(Eu_{1-x}Ca_x)_3In_2Ge_3$ [10], which only exist when mixed

cations are present, despite the fact that the latter are in the same valence state (n.b., Eu and Yb are nominally divalent in these structures). Finally, attesting to the competition between electronic and geometric considerations in germanides, are the structures of $(Eu_xCa_{1-x})_2Ge_2Pb$ (space group *Pbam*) and $(Eu_xSr_{1-x})_2Ge_2Pb$ (space group *Cmmm*) [11]. Both structures boast anionic sub-lattices with fully ordered Ge and Pb at the atomic level, which is unusual for elements of the same group, yet, as evident from the different space groups, have not only different global symmetry, but also different arrangements of Ge and Pb atoms—all of which is apparently governed by the small differences in electronegativity and atomic sizes between Ca and Sr [16].

Here, we report three compounds that were identified over the course of the previous studies, namely $Sr_xCa_{1-x}Al_2Ge_2$ ($x \approx 0.4$) and $SrAl_2Ge_2$, as well as the binary calcium germanide CaGe. Although not all new phases ($SrAl_2Ge_2$ and CaGe have been known for decades), to date, their crystal structures have not been established from single-crystal X-ray diffraction methods.

2. Materials and Methods

The synthesis followed the established procedures for $SrAl_{4-x}Ge_x$ [4], $M_3In_2Ge_4$ and $M_5In_3Ge_6$ (M = Ca, Sr, Eu, and Yb) [9], and $(Eu_xCa_{1-x})_2Ge_2Pb$ [11] described in detail in the respective publications. We are not repeating the experimental details here since the title compounds were identified as side products of analogous exploratory reactions. The reader is also referred to the earlier works on polycrystalline $SrAl_2Ge_2$ and CaGe, where phase pure samples have been obtained [17–22]. In this paper, we will only emphasize that all manipulations were performed inside a glovebox under the inert atmosphere of argon (with oxygen and moisture levels below 1 ppm) or vacuum. The starting materials were used as received (>99.9 wt%). After the completion of the reactions, the products were extracted and brought back into the glove box. The crystals were small and had irregular morphologies. Air stability was not checked explicitly, although by visual appearance the samples appear to react with air (or moisture) very rapidly. X-ray powder diffraction patterns were not taken, either, since efforts to synthesize the compounds in quantitative yields were not undertaken.

Single crystals were selected under dry Paratone-N oil and cut to the desired dimensions (around 0.1 mm or less) with a scalpel. Multiple crystals had to be tried before the ones with the best quality were identified. Intensity data were collected at 200 K on a Bruker SMART CCD diffractometer. The data collection was carried out at different ω and θ angles with a frame width of 0.8° along with 6–10 sec counting time. SMART and SAINT software [23,24] were used to collect the raw data and to integrate the measured reflections. Absorption correction was applied using SADABS [25]. The structures are known [17–22], and the atomic coordinates were taken from the literature. Refinements by least-square minimizations on F^2 were carried out with the aid of the SHELXL package [26]. The atomic coordinates from the previous reports on these germanide phases were suitable starting models. The first refinement cycles quickly converged to low conventional residual factors and led to featureless difference Fourier maps in all cases except $Sr_xCa_{1-x}Al_2Ge_2$. In the latter case, the unphysical site occupation factor (SOF) of the Ca site suggested that randomly disordered Ca and Sr atoms must be considered in that position in order to achieve proper fitting. The final refinement was done with a constraint on the displacement parameters for Ca/Sr (EADP in SHELXL [26]), which yielded a statistical distribution of Ca and Sr in a ratio of approximately 2:1, giving a final refined formula of $Sr_xCa_{1-x}Al_2Ge_2$ (x = 0.36(1)).

Details of the data collection and selected crystallographic parameters are summarized in Tables 1 and 2.

Table 1. Selected single-crystal data collection and structure refinement parameters for CaGe, $SrAl_2Ge_2$, and $Sr_xCa_{1-x}Al_2Ge_2$ ($x \approx 0.4$).

Empirical Formula	CaGe	$SrAl_2Ge_2$	$Sr_{0.36(1)}Ca_{0.64}Al_2Ge_2$
Formula weight	112.67	286.76	256.33
Temperature (K)	200(2)	200(2)	200(2)
Radiation, λ	Mo Kα, 0.71073 Å	Mo Kα, 0.71073 Å	Mo Kα, 0.71073 Å
Space group, Z	*Cmcm*, 4	$P\bar{3}m1$, 1	$P\bar{3}m1$, 1
a (Å)	4.5698(8)	4.2157(13)	4.1929(3)
b (Å)	10.832(2)	-	-
c (Å)	3.9979(8)	7.443 (3)	7.2810(12)
V (Å^3)	197.90(6)	114.55(7)	110.85(2)
ρ_{cal} (g/cm^3)	3.78	4.16	3.84
μ (cm^{-1})	175.2	248.1	187.6
Goodness-of-fit on F^2	1.084	1.135	1.282
Unique reflections	157	136	151
Refined parameters	10	9	11
R_1 ($I > 2\sigma_I$) [a]	0.0222	0.0304	0.0155
wR_2 ($I > 2\sigma_I$) [a]	0.0501	0.0675	0.0367
R_1 (all data) [a]	0.0233	0.0432	0.0159
wR_2 (all data) [a]	0.0507	0.0722	0.0369
Largest diff. peak andhole (e^-/Å^3)	0.57 and −0.87	1.83 and −0.86	0.46 and −0.69

[a] $R_1 = \sum||F_o| - |F_c|| / \sum|F_o|$; $wR_2 = [\sum[w(F_o^2 - F_c^2)^2] / \sum[w(F_o^2)^2]]^{1/2}$, where $w = 1/[\sigma^2 F_o^2 + (AP)^2 + (BP)]$ and $P = (F_o^2 + 2F_c^2)/3$. A and B are the respective weight coefficients (see the CIFs).

Table 2. Atomic coordinates of the atoms and their equivalent isotropic displacement parameters U_{eq} [a] for CaGe, $SrAl_2Ge_2$, and $Sr_xCa_{1-x}Al_2Ge_2$ ($x \approx 0.4$).

Atom	Site	x	y	z	U_{eq} (Å^2)
		CaGe			
Ca	4*c*	0	0.0763(1)	1/4	0.010(1)
Ge	4*c*	0	0.3622(1)	1/4	0.010(1)
		$SrAl_2Ge_2$			
Sr	1*a*	0	0	0	0.014(1)
Al	2*d*	2/3	1/3	0.3738(5)	0.013(1)
Ge	2*d*	1/3	2/3	0.2724(2)	0.014(1)
		$Sr_{0.36(1)}Ca_{0.64}Al_2Ge_2$			
Ca/Sr [b]	1*a*	0	0	0	0.010(1)
Al	2*d*	1/3	2/3	0.3719(1)	0.010(1)
Ge	2*d*	2/3	1/3	0.2656(2)	0.009(1)

[a] U_{eq} is defined as one-third of the trace of the orthogonalized U_{ij} tensor. [b] Refined occupancies for Ca/Sr = 0.643(5)/0.357.

3. Results and Discussion

3.1. Structure of CaGe

CaGe crystallizes with the well-known orthorhombic CrB-type (space group *Cmcm* (no. 63); $Z = 4$; Pearson symbol *o*C8) [27]. The structure type is also often referred to as AlTh. This relatively simple structure, with just two positions in the asymmetric unit, has received much attention in the past, and will not be discussed in detail in this paper. A schematic structural representation is given in Figure 1.

As stated earlier, the binary CaGe phase is known, and its structure has been correctly assigned to the CrB-type based on earlier work [19–22]. However, this is the first time the structure is refined, and accurate values for the atomic coordinates and the atomic displacement parameters become available. We note that the metrics of the unit cell reported here (Table 1) are in excellent agreement with the earlier reported unit cell parameters from powder X-ray diffraction. The small and systematic decrease of the *a*-, *b*-, and *c*-lattice

vectors is due to the lower temperature of the single-crystal X-ray diffraction experiment (200 K vs room temperature for the powder work).

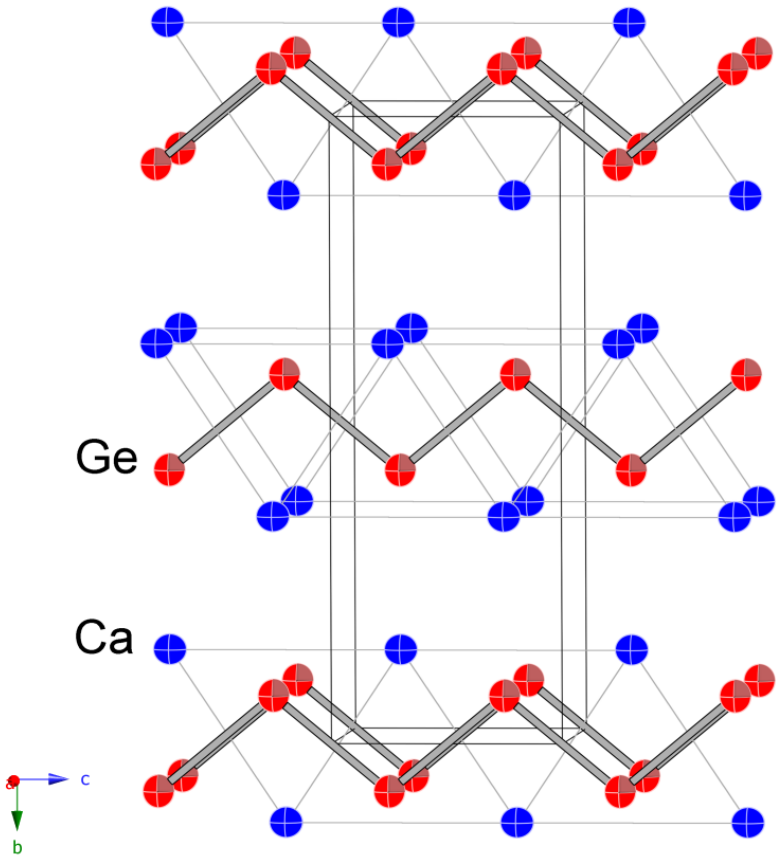

Figure 1. Off [100]-view of the crystal structure of CaGe, emphasizing the Ge zigzag chains and the packing of the metal-atom polyhedra. The unit cell is outlined. Thermal ellipsoids are drawn at the 95% probability level.

As can be gathered from the crystal structure representation of CaGe in Figure 1, the best way to describe it is as an array of fused trigonal prisms of Ca atoms that are centered by Ge atoms. The open "square" faces of the trigonal prisms are capped by another Ca from adjacent slabs, but those contacts are not depicted in Figure 1 for clarity. Also, as emphasized in Figure 1, the Ge atoms interact with one another, forming infinite zigzag chains. The chains propagate along the crystallographic *c*-axis and are stacked along the crystallographic *b*-axis.

According to the refinements, the Ge–Ge distance is 2.5934(9) Å (Table 3). Generally speaking, 2.59 Å is a long bond, considering that the Pauling (single-bonded) radius of Ge is 1.24 Å [16]. However, this value matches very well with the experimentally determined Ge–Ge distances in a number of other binary and ternary alkaline-earth or rare-earth germanides such as $CaGe_2$ [1], Sm_3Ge_5 [2], Ca_4InGe_4 [3], $RE_{5-x}Ca_xGe_4$ [13,28], $RE_{5-x}Ca_xGe_3$ [14,15] $RE_{5-x}Li_xGe_4$ [29], $RE_{5-x}Mg_xGe_4$ [30], RE_2MgGe_2 [31], $Sr_3Cd_8Ge_4$ [32], and the members of the homologous series $[REGe_2]_n[RELi_2Ge]_m$ [33–35], among others. An excellent benchmark case is the structure of Ca_5Ge_3 [36,37], where some of the Ge atoms are dimerized. The length of the Ge–Ge bond in Ca_5Ge_3 measures 2.575 Å. If one were to assume the bonding within the Ge_2-dimers to be akin to 2-center-2-electron bonds (i.e., $[Ge_2]^{6-}$ is isoelectronic with the Br_2 molecule), then applying the Zintl concept [38] to the binary Ca_5Ge_3 compound would lead to the formulation $(Ca^{2+})_5([Ge_2]^{6-})(Ge^{4-})$. Doing the same for CaGe means the infinite zigzag chains of Ge atoms would be considered as each Ge atom in a 2-bonded configuration and needing two additional electrons to fulfill

the octet. Therefore, the Ge atoms in CaGe will bear a formal charge "2−", which means that the structure is perfectly electron-balanced, i.e., $Ca^{2+}Ge^{2-}$.

Table 3. Selected interatomic distances (Å) in CaGe. Only the shortest Ca–Ca contacts are shown, the rest are 3.9 Å and longer.

Atom Pair	Distance
Ge–Ge (×2)	2.5934(9)
Ge–Ca	3.098(2)
Ge–Ca (×4)	3.1082(5)
Ge–Ca (×2)	3.255(1)
Ca–Ca (×2)	3.593(2)

Evidently, this simplified bonding picture of a salt-like solid provides an easy way to partition the valence electrons, predicting intrinsic semiconducting behavior. The properties of CaGe are also computationally predicted and available from the Materials Project [39]. To our knowledge, there is no experimental validation of this supposition. We need to recall that the Zintl phase Ca_5Ge_3 is known to be a metallic conductor, and Mudring and Corbett have shown the importance of the overlap of empty Ca 3d states with Ge 4p states, which is not captured by the Zintl formalism [37]. Effectively, this means that what we assigned above to be a bond of a single bond-order is not representative of the actual bonding picture, which is more akin to a partial double bond. This may be the case here as well, and CaGe may show metallicity, calling for further and more detailed investigation. Considering the anisotropy of the structure, it may also be suggested that an eventual conduction mechanism could manifest itself in a specific orientation only.

The respective Ca–Ge contacts are in the range of ca. 3.10 Å to ca. 3.25 Å (Table 3). The Ca–Ge in distances are generally slightly longer than the sum of the Pauling (single-bonded) radii of Ca, and Ge atoms (e.g., $r_{Ca} + r_{Ge}$ = 2.99 Å) [16]; this is suggestive of some directional bonding between these types of atoms. All identified metrics regarding the distances are comparable with those of related germanide systems [1,3,9,36].

Metal–metal bonding also appears to be present, as evidenced by the interactions in the ca. 3.6 Å range. Such metal–metal interactions, although not as extensive as in other systems, are expected to influence the electronic structure, and indeed, have been shown to contribute to the metallic character of the above-mentioned Ca_5Ge_3 phase.

3.2. Structures of $SrAl_2Ge_2$, and $Sr_xCa_{1-x}Al_2Ge_2$ ($x \approx 0.4$)

$Sr_xCa_{1-x}Al_2Ge_2$ ($x \approx 0.4$) and $SrAl_2Ge_2$ crystallize with the $CaAl_2Si_2$-type structure in the trigonal space group $P\bar{3}m1$ (no. 164; Z = 1; Pearson symbol $hP5$) [27]. The structure type is also often referred to as anti-La_2O_3 or anti-Ce_2O_2S. This relatively simple structure, with three atomic positions in the asymmetric unit (Table 2), has received much attention in the past [17,18,40–45] and will not be discussed in detail in this paper. A schematic structural representation is given in Figure 2.

As stated earlier, the ternary $SrAl_2Ge_2$ phase has been known since 1967 [17], and its structure has been correctly assigned to the $CaAl_2Si_2$-type based on powder X-ray diffraction [17]. In 2019, a report on $SrAl_2Ge_2$ refined by the Rietveld method appeared [18]. However, the current work is the first time the structure is refined from single-crystal X-ray diffraction data. We note that the metrics of the unit cell reported here (Table 1) are in excellent agreement with the 1967 report, which gives unit cell parameters a = 4.225 Å and c = 7.448 Å. Similar to the case of CaGe (vide supra), the small and systematic decrease of the a- and c-lattice vectors we report is due to the lower temperature of the single-crystal X-ray diffraction experiment (200 K vs room temperature for the powder work). However, our reported metrics (a = 4.216 Å and c = 7.443 Å) are much lower than those from the 2019 paper (a = 4.234 Å and c = 7.481 Å) [18], which may suggest that there are potential small structural variations in some of the samples that come about from the purity of the materials being used for the synthesis and/or the synthetic protocols. We also note that

the isotropic displacement parameters from the Rietveld refinements for $SrAl_2Ge_2$ show U_{eq} of the Al atom nearly twice the size of U_{eq} of the Ge atom [18], while the displacement parameters listed in Table 2 from the refinements for $SrAl_2Ge_2$ display nearly equal values.

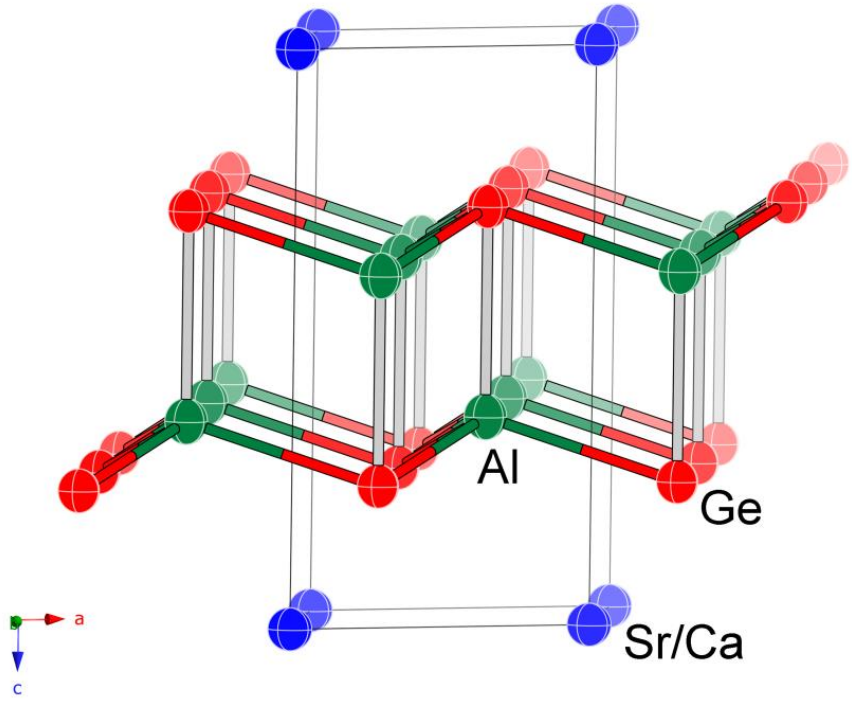

Figure 2. Off [010]-view of the crystal structure of $Sr_{0.36(1)}Ca_{0.64}Al_2Ge_2$, emphasizing the double $[Al_2Ge_2]^{2-}$ layers. The three shorter and one longer Al–Ge bonds are represented with different colors. The unit cell is outlined. Thermal ellipsoids are drawn at the 95% probability level.

We also note that the ternary $CaAl_2Ge_2$ phase has also been known since 1967 [17], and its structure has been correctly assigned to the $CaAl_2Si_2$-type based on powder X-ray diffraction. The $CaAl_2Ge_2$ structure has been refined from single-crystal X-ray diffraction data in two independent publications in 2001 and 2002 [40,41]. The *a*- and *c*-lattice vectors in the latter reports are in excellent agreement. Here, we report for the first time the structure of $Sr_xCa_{1-x}Al_2Ge_2$ ($x \approx 0.4$), which is a new compound. Its composition indicates a ca. 2:1 solid solution of $CaAl_2Ge_2$ and $SrAl_2Ge_2$. While we did not attempt to study the full solubility range, it is reasonable to suggest that $Sr_xCa_{1-x}Al_2Ge_2$ ($0 \leq x \leq 1$) will exist, given that both end members are known and stable phases.

As stated above, the structure is best described as double corrugated $[Al_2Ge_2]^{2-}$ layers. These 2D fragments are built through corner- and edge-shared tetrahedra as shown in Figure 2. Such a polyanionic network can be derived by puckering of "dimerized" honeycomb layers or by splitting of wurtzite-type 3D lattice, followed by a subsequent reconstruction [42–45]. Divalent cations, Ca^{2+}, and/or Sr^{2+} fill the space between neighboring layers; they have coordination number 6 (slightly distorted octahedra formed by Ge atoms).

As seen from Figure 2, the Ge atoms have a hexagonal closed-packed arrangement, in which the Al atoms occupy half of the tetrahedral holes and the alkaline-earth atoms occupy half of the octahedral holes. A filled variant of the $CaAl_2Si_2$-type structure is known, exemplified by $CeLi_3Sb_2$ and related pnictides (Pearson symbol *hP*6), where additional Li atoms reside in the other half of the octahedral voids (with fractional coordinates 0, 0, 1/2) [46].

All relevant distances are compiled in Table 4. Of note are two specific observations. First are the subtle distortions of the formed $AlGe_4$-tetrahedra. Comprehensive theoretical studies from Zheng et al. [42,43] discuss the differences between the "rib" and the "handle"

bonds in this structure from a molecular orbitals' viewpoint, and the reader is referred to it for further information. Second is the accuracy and precision of the herein-reported refined structure of $SrAl_2Ge_2$. For comparison, the 1967 report [17], puts the Al and Ge atoms at distances of 2.562 Å and 2.719 Å, the latter being very far off from the herein-discussed 2.633 (4) Å.

Table 4. Selected interatomic distances (Å) in $SrAl_2Ge_2$ and $Sr_{0.36(1)}Ca_{0.64}Al_2Ge_2$. Shortest metal–metal contacts are equal to the *a*-lattice vector (longer than 4.2 Å) and are not shown.

Atom Pair	Distance	Atom Pair	Distance
$SrAl_2Ge_2$		$Sr_{0.36(1)}Ca_{0.64}Al_2Ge_2$	
Ge–Al (×3)	2.548(2)	Ge–Al (×3)	2.5415(5)
Ge–Al	2.633(4)	Ge–Al	2.639(1)
Sr–Ge (×6)	3.168(1)	Sr/Ca–Ge (×6)	3.0984(4)
Sr–Al (×6)	3.697(3)	Sr/Ca–Al (×6)	3.632(1)

The refined Al–Ge distances in both $SrAl_2Ge_2$ and $Sr_{0.36(1)}Ca_{0.64}Al_2Ge_2$ are slightly longer than the sum of the Pauling (single-bonded) radii of Al and Ge atoms (e.g., $r_{Al} + r_{Ge}$ = 2.49 Å) [16], but are comparable with those of related alumo-germanide systems [4,5,7,8,39,40]. This is suggestive of the strong covalent bonding between these atoms in the structure. One may notice that upon contraction of the unit cell from $SrAl_2Ge_2$ to $Sr_{0.36(1)}Ca_{0.64}Al_2Ge_2$, the "rib" and the "handle" bonds respond differently—the former becomes slightly shorter, while the latter becomes slightly longer.

The Sr–Ge and Sr/Ca–Ge distances also match very well the sum of the respective Pauling (single-bonded) radii of Sr, Ca, and Ge atoms (e.g., $r_{Ca} + r_{Ge}$ = 2.99 Å; $r_{Sr} + r_{Ge}$ = 3.15 Å) [16], which also indicates some directional bonding between these types of atoms. The Sr–Al and Sr/Ca–Al distances are much longer than the sum of the respective Pauling radii, suggestive of much weaker interactions between these types of atoms. The contraction of the unit cell on going from $SrAl_2Ge_2$ to $Sr_{0.36(1)}Ca_{0.64}Al_2Ge_2$ scales very well with the distances in question.

Lastly, a few brief words on the electronic structure and the valence electron count in $SrAl_2Ge_2$ and $Sr_{0.36(1)}Ca_{0.64}Al_2Ge_2$. There have been numerous prior reports on the electronic structures of compounds adopting the $CaAl_2Si_2$ structure [42–45]. The properties of $CaAl_2Ge_2$ are also computationally predicted and available from the Materials Project [47]. Almost exclusively, all compounds with the $CaAl_2Si_2$ structure can be easily rationalized by the Zintl-Klemm concept [38] ss perfectly electron-balanced, i.e., as Zintl phases. Considering the structural representation in Figure 2 with polyanionic double $[Al_2Ge_2]^{2-}$ layers (the formal charge "2−" comes about from the 4 covalent bonds of the Al atoms, which only have 3 valence electrons and need one additional to fill their 3p sub-shells), the formula can be partitioned as $M^{2+}[Al_2Ge_2]^{2-}$. The already-mentioned study from Zheng et al. [42,43] has also shown that the $CaAl_2Si_2$ structure is fully optimized with 16 valence electrons per formula unit and most compounds, which adopt this structure type meet this criterion. Numerous papers with band structure calculations of related structures have shown that there are typically eight bands below the Fermi level, which corresponds to the discussed 16 valence electrons for $SrAl_2Ge_2$ [2(Sr) + 2 × 3(Al) + 2 × 4(Ge) = 16). However, just as was the case with the previously mentioned binary compound Ca_5Ge_3 [37], care needs to be exercised when $SrAl_2Ge_2$ and $Sr_{0.36(1)}Ca_{0.64}Al_2Ge_2$ are assigned as Zintl phases (and expected to be semiconductors)—the reason for this cautionary remark comes from the physical property studies of the isostructural silicides $CaAl_2Si_2$ and $SrAl_2Si_2$, which are shown to be semimetals [48–51].

Author Contributions: Conceptualization, N.-T.S. and S.B.; formal analysis, N.-T.S. and S.B.; investigation, N.-T.S.; writing—original draft preparation, S.B.; writing—review and editing, S.B.; project administration, S.B.; funding acquisition, S.B. All authors have read and agreed to the published version of the manuscript.

Funding: This work was supported by the US National Science Foundation, grants DMR-0743916 (CAREER) and DMR-2004579.

Institutional Review Board Statement: Not applicable.

Informed Consent Statement: Not applicable.

Data Availability Statement: The corresponding crystallographic information files (CIF) have been deposited with the Cambridge Crystallographic Database Centre (CCDC) and can be obtained free of charge via http://www.ccdc.cam.ac.uk/conts/retrieving.html (accessed on 10 October 2022) (or from the CCDC, 12 Union Road, Cambridge CB2 1EZ, UK; Fax: +44-1223-336033; E-mail: deposit@ccdc.cam.ac.uk) with the following depository numbers: 2211492–2211494.

Acknowledgments: The authors are indebted to K. Ghosh for proof reading the manuscript and for useful discussions.

Conflicts of Interest: The authors declare no conflict of interest.

References

1. Tobash, P.H.; Bobev, S. Synthesis, structure and electronic structure of a new polymorph of $CaGe_2$. *J. Solid State Chem.* **2007**, *180*, 1575–1581. [CrossRef]
2. Tobash, P.H.; Lins, D.; Bobev, S.; Hur, N.; Thompson, J.D.; Sarrao, J.L. Vacancy ordering in $SmGe_{2-x}$ and $GdGe_{2-x}$ (x = 0.33): Properties of two Sm_3Ge_5 polymorphs and of Gd_3Ge_5. *Inorg. Chem.* **2006**, *45*, 7286–7294. [CrossRef] [PubMed]
3. You, T.-S.; Jung, Y.; Bobev, S. Experimental and theoretical investigations of the novel ternary compound Ca_4InGe_4. *Dalton Trans.* **2012**, *41*, 12446–12451. [CrossRef] [PubMed]
4. Zhang, J.; Bobev, S. Synthesis, Structural Characterization and Properties of $SrAl_{4-x}Ge_x$, $BaAl_{4-x}Ge_x$, and $EuAl_{4-x}Ge_x$ ($x \approx$ 0.3–0.4)—Rare examples of electron-rich phases with the $BaAl_4$ structure type. *J. Solid State Chem.* **2013**, *205*, 21–28. [CrossRef]
5. Zhang, J.; Liu, Y.; Shek, C.H.; Wang, Y.; Bobev, S. On the structures of the rare-earth metal germanides from the series $REAl_{1-x}Ge_3$ (RE = Nd, Sm, Gd, Tb, Dy, Ho; 0.6 <x <0.9). A tale of vacancies at the Al Sites and the concomitant structural modulations. *Dalton Trans.* **2017**, *46*, 9253–9265. [PubMed]
6. Tobash, P.H.; Lins, D.; Bobev, S.; Lima, A.; Hundley, M.F.; Thompson, J.D.; Sarrao, J.L. Crystal growth, structural, and property studies on a family of ternary rare-earth phases RE_2InGe_2 (RE = Sm, Gd, Tb, Dy, Ho, Yb). *Chem. Mater.* **2005**, *17*, 5567–5573. [CrossRef]
7. Zhang, J.; Bobev, S. Correlations between chemical bonding and magnetic exchange interactions: Synthesis, crystal structures, and magnetic properties of the new family RE_2AlGe_2 (RE = Tb–Tm, Lu). *Inorg. Chem.* **2013**, *52*, 5307–5315. [CrossRef]
8. Zhang, J.; Wang, Y.; Bobev, S. Structural modulations in the rare-earth metal digermanides $REAl_{1-x}Ge_2$ (RE = Gd−Tm, Lu, Y; 0.8 <x <0.9). Correlations between long- and short-range vacancy ordering. *Inorg. Chem.* **2015**, *54*, 722–732.
9. You, T.-S.; Bobev, S. Synthesis and structural characterization of $A_3In_2Ge_4$ and $A_5In_3Ge_6$ (A = Ca, Sr, Eu, Yb)—New intermetallic compounds with complex structures, exhibiting Ge–Ge and In–In bonding. *J. Solid State Chem.* **2010**, *183*, 1258–1265. [CrossRef]
10. You, T.-S.; Tobash, P.H.; Bobev, S. Mixed cations and structural complexity in $(Eu_{1-x}Ca_x)_4In_3Ge_4$ and $(Eu_{1-x}Ca_x)_3In_2Ge_3$—The first two members of the homologous series $A_{2[n+m]}In_{2n+m}Ge_{2[n+m]}$ (n, m = 1,2 . . . ∞; A = Ca, Sr, Ba, Eu, or Yb). *Inorg. Chem.* **2010**, *49*, 1773–1783. [CrossRef]
11. Suen, N.-T.; Hooper, J.; Zurek, E.; Bobev, S. On the nature of Ge−Pb bonding in the solid state. Synthesis, structural characterization, and electronic structures of two unprecedented germanide-plumbides. *J. Am. Chem. Soc.* **2012**, *134*, 12708–12716. [CrossRef] [PubMed]
12. Tobash, P.H.; Bobev, S.; Ronning, F.; Thompson, J.D.; Sarrao, J.L. Structural chemistry and magnetic properties of $RE_2[Sn_xGe_{1-x}]_5$ (RE = Nd, Sm) and $RE[Sn_xGe_{1-x}]_2$ (RE = Gd, Tb): Four new rare-earth metal intermetallic compounds with germanium zig-zag chains and tin square-nets. *J. Alloy. Compd.* **2009**, *488*, 511. [CrossRef]
13. Suen, N.-T.; Bobev, S. Calcium substitution in rare-earth metal germanides with the Gd_5Si_4 type structure. *Z. Anorg. Allg. Chem.* **2022**, *648*, e202200016. [CrossRef]
14. Suen, N.-T.; Bobev, S. Calcium substitution in rare-earth metal germanides with the Cr_5B_3 type structure. *Z. Anorg. Allg. Chem.* 2022, in print.
15. Suen, N.-T.; Broda, M.; Bobev, S. Calcium substitution in rare-earth metal germanides with the hexagonal Mn_5Si_3 structure type. Structural characterization of the extended series $RE_{5-x}Ca_xGe_3$ (RE = rare-earth metal). *J. Solid State Chem.* **2014**, *217*, 142–149. [CrossRef]
16. Pauling, L. *The Nature of the Chemical Bond*, 3rd ed.; Cornell University Press: Ithaca, NY, USA, 1960.

17. Gladishevskij, E.J.; Kripjakevic, P.I.; Bodak, O.I. The crystal structures of the compound $CaAl_2Si_2$ and its analogues. *Ukr. Fiz. Zh. (Russ. Ed.)* **1967**, *12*, 447–453.
18. Shi, X.-M.; Chen, L.-Q.; He, H.; Sun, Y.-X.; Zeng, Z.; Tang, J. Investigation on the preparation and thermoelectric properties of layered $SrAl_2Ge_2$. *J. Sichuan Univ. (Nat. Sc. Ed)* **2019**, *56*, 940–943.
19. Schob, O.; Parthé, E. AB Compounds with Sc, Y and rare earth metals. I. Scandium and Yttrium Compounds with CrB and CsCl Structure. *Acta Crystallogr.* **1965**, *19*, 214–224. [CrossRef]
20. Merlo, F.; Europa, C. The Pseudobinary systems $SrAg_{1-x}Zn_x$, $CaCu_{1-x}Ga_x$ and $CaCu_{1-x}Ge_x$ and their use for testing structural maps. *J. Less Common Met.* **1986**, *119*, 45–61. [CrossRef]
21. Iandelli, A. Legami covalenti nei composti intermetallici. I composti PrGe e CaGe. *Atti Della Accad. Naz. Dei Lincei Cl. Di Sci. Fis. Mat. E Nat. Rend.* **1955**, *19*, 307–313.
22. Palezona, A.; Manifretti, P.; Fornasini, M.L. The phase diagram of the Ca–Ge system. *J. Alloy. Compd.* **2002**, *345*, 144–147. [CrossRef]
23. *SMART*, version 2.10; Bruker Analytical X-ray Systems, Inc.: Madison, WI, USA, 2003.
24. *SAINT*, version 6.45; Bruker Analytical X-ray Systems, Inc.: Madison, WI, USA, 2003.
25. *SADABS*, version 2.10; Bruker Analytical X-ray Systems, Inc.: Madison, WI, USA, 2003.
26. Sheldrick, G.M. Crystal structure refinement with *SHELXL*. *Acta Crystallogr. C* **2015**, *71*, 3–8. [CrossRef] [PubMed]
27. Villars, P.; Calvert, L.D. (Eds.) *Pearson's Handbook of Crystallographic Data for Intermetallic Compounds*, 2nd ed.; American Society for Metals: Materials Park, OH, USA, 1991.
28. Wu, L.-M.; Kim, S.-H.; De, D.-K.S. Electron-precise/deficient $La_{5-x}Ca_xGe_4$ ($3.4 < x < 3.8$) and $Ce_{5-x}Ca_xGe_4$ ($3.0 < x < 3.3$): Probing low-valence electron concentrations in metal-rich Gd_5Si_4-type germanides . *J. Am. Chem. Soc.* **2015**, *127*, 15682–15683.
29. Suen, N.-T.; You, T.-S.; Bobev, S. Synthesis, crystal structures and chemical bonding of $RE_{5-x}Li_xGe_4$ (*RE* = Nd, Sm and Gd; $x \simeq 1$) with the orthorhombic Gd_5Si_4 Type. *Acta Crystallogr. C* **2013**, *69*, 1–4. [CrossRef] [PubMed]
30. Tobash, P.H.; Bobev, S.; Thompson, J.D.; Sarrao, J.L. Magnesium substitutions in rare-earth metal germanides with the orthorhombic Gd_5Si_4-type structure. Synthesis, crystal chemistry, and magnetic properties of $RE_{5-x}Mg_xGe_4$ [*RE* = Gd–Tm, Lu, and Y]. *Inorg. Chem.* **2009**, *48*, 6641–6651. [CrossRef] [PubMed]
31. Suen, N.-T.; Tobash, P.H.; Bobev, S. Synthesis, structural characterization and magnetic properties of RE_2MgGe_2 (*RE* = rare-earth metal). *J. Solid State Chem.* **2011**, *184*, 2941–2947. [CrossRef]
32. Guo, S.-P.; Meyers, J.J.; Tobash, P.H.; Bobev, S. Eleven new compounds in the *RE*-Cd-Ge systems (*RE* = Pr, Nd, Sm, Gd–Yb; Y): Crystal chemistry of the RE_2CdGe_2 series. *J. Solid State Chem.* **2012**, *192*, 16–22. [CrossRef]
33. Suen, N.-T.; Huang, L.; Meyers, J.J.; Bobev, S. An Unusual triple-decker variant of the tetragonal $BaAl_4$-structure type: Synthesis, structural characterization, and chemical bonding of $Sr_3Cd_8Ge_4$ and $Eu_3Cd_8Ge_4$. *Inorg. Chem.* **2018**, *57*, 833–842. [CrossRef]
34. Guo, S.-P.; You, T.-S.; Bobev, S. Closely related rare-earth metal germanides $RE_2Li_2Ge_3$ and $RE_3Li_4Ge_4$ (*RE* = La–Nd, Sm): Synthesis, crystal chemistry, and magnetic properties. *Inorg. Chem.* **2012**, *51*, 3119–3129. [CrossRef]
35. Guo, S.-P.; You, T.-S.; Jung, Y.; Bobev, S. Synthesis, crystal chemistry, and magnetic properties of $RE_7Li_8Ge_{10}$ and $RE_{11}Li_{12}Ge_{16}$ (*RE* = La−Nd, Sm): New members of the $[REGe_2]_n[RELi_2Ge]_m$ homologous series. *Inorg. Chem.* **2012**, *51*, 6821–6829. [CrossRef]
36. Eisenmann, B.; Schäfer, H. The crystal structures of Ca_5Si_3 and Ca_5Ge_3. *Z. Naturforsch. B* **1974**, *29*, 460–463. [CrossRef]
37. Mudring, A.V.; Corbett, J.D. Unusual electronic and bonding properties of the Zintl phase Ca_5Ge_3 and related compounds. *A theoretical analysis. J. Am. Chem. Soc.* **2004**, *126*, 5277–5281. [CrossRef] [PubMed]
38. Nesper, R. The Zintl-Klemm concept—A historical survey. *Z. Anorg. Allg. Chem.* **2014**, *640*, 2639–2648. [CrossRef]
39. The Materials Project. *Materials Data on CaGe by Materials Project*; USA, 2020; N. p. Web. [CrossRef]
40. Kranenberg, C.; Johrendt, D.; Mewis, A. The stability range of the $CaAl_2Si_2$-type structure in case of $LnAl_2Ge_2$ compounds. *Solid State Sci.* **2002**, *4*, 261–265. [CrossRef]
41. Carrillo-Cabrera, W.; Gil, R.C.; Grin, Y. Refinement of the crystal structure of monocalcium dialuminide digermanide, $Ca[Al_2Ge_2]$. *Z. Krist.—New Cryst. Struct.* **2001**, *216*, 535–536. [CrossRef]
42. Zheng, C.; Hoffmann, R. Complementary local and extended views of bonding in the $ThCr_2Si_2$ and $CaAl_2Si_2$ structures. *J. Solid State Chem.* **1988**, *72*, 58–71. [CrossRef]
43. Zheng, C.; Hoffmann, R.; Nesper, R.; von Schnering, H.-G. Site preferences and bond length differences in $CaAl_2Si_2$ type Zintl compounds. *J. Am. Chem. Soc.* **1986**, *108*, 1876–1884. [CrossRef]
44. Peng, W.; Chanakian, S.; Zevalkink, A. Crystal chemistry and thermoelectric transport of layered AM_2X_2 compounds. *Inorg. Chem. Front.* **2018**, *5*, 1744–1759. [CrossRef]
45. Burdett, J.K.; Miller, G.J. Fragment formalism in main-group solids: Applications to AlB_2, $CaAl_2Si_2$, $BaAl_4$ and related materials. *Chem. Mater.* **1990**, *2*, 12–26. [CrossRef]
46. Schäfer, M.C.; Suen, N.-T.; Raglione, M.; Bobev, S. The layered antimonides $RELi_3Sb_2$ (*RE* = Ce–Nd, Sm, Gd–Ho). Filled derivatives of the $CaAl_2Si_2$ structure type. *J. Solid State Chem.* **2014**, *210*, 89–95. [CrossRef]
47. The Materials Project. *Materials Data on Ca(AlGe)2 by Materials Project*; USA, 2020; N. p. Web. [CrossRef]
48. Strikos, S.; Joseph, B.; Alabarse, F.G.; Valadares, G.; Costa, D.G.; Capaz, R.B.; ElMassalami, M. Structural metastability and Fermi surface topology of $SrAl_2Si_2$. *Inorg. Chem.* **2021**, *60*, 18652–18661. [CrossRef]
49. Kauzlarich, S.M.; Condron, C.L.; Wassei, J.K.; Ikeda, T.; Snyder, G.J. Structure and high-temperature thermoelectric properties of $SrAl_2Si_2$. *J. Solid State Chem.* **2009**, *182*, 240–245. [CrossRef]

50. Zevalkink, A.; Bobnar, M.; Schwarz, U.; Grin, Y. Making and braking bonds in superconducting $SrAl_{4-x}Si_x$ (0 <x <2). *Chem. Mater* **2017**, *29*, 1236–1244.
51. Imai, M.; Abe, H.; Yamada, K. Electrical properties of single-crystalline $CaAl_2Si_2$. *Inorg. Chem.* **2004**, *43*, 5186–5188. [CrossRef] [PubMed]